J Mater Sci (2010) 45:1272–1279
DOI 10.1007/s10853-009-4078-3

Electronic characterization and photocatalytic properties of TiO_2/CdO electrospun nanofibers

Muzafar A. Kanjwal · Nasser A. M. Barakat · Faheem A. Sheikh · Hak Yong Kim

Received: 16 October 2009 / Accepted: 24 November 2009 / Published online: 10 December 2009

Abstract Titanium dioxide-cadmium oxide (TiO_2/CdO) nanofibers were prepared by the electrospinning technique followed by a single-step calcination from a solution of titanium isopropoxide and cadmium acetate dihydrate. Scanning electron microscopy, transmission electron microscopy, and the Brunauer–Emmett–Teller technique were employed to characterize the as-spun nanofibers as well as the calcined product. The specific surface area of the calcined product was calculated to be 65.3067 $m^2\ g^{-1}$. X-ray powder diffractometry analysis was conducted on the samples to study their chemical composition as well as their crystallographic structure. The results obtained indicated that the prepared nanostructure product can eliminate all of the methyl orange dye within about 75 min, whereas the pristine titanium dioxide nanofibers could not eliminate more than 50% even after 180 min.

M. A. Kanjwal
Department of Polymer Nano Science and Technology, Chonbuk National University, Jeonju 561-756, Republic of Korea

N. A. M. Barakat
Chemical Engineering Department, Faculty of Engineering, El-Minia University, El-Minia, Egypt

N. A. M. Barakat (✉) · F. A. Sheikh
Bionano System Engineering, Chonbuk National University, Jeonju 561-756, Republic of Korea
e-mail: nasbarakat@yahoo.com

H. Y. Kim (✉)
Department of Textile Engineering, Chonbuk National University, Jeonju 561-756, Republic of Korea
e-mail: khy@chonbuk.ac.kr; kanjwalmuzafar@gmail.com

Introduction

Titanium dioxide is known to be the most effective photocatalyst and has attracted a great deal of attention in various fields due to its numerous technological applications [1, 2]. Titanium dioxide has proven to be an attractive and promising catalyst in heterogeneous photocatalysis and in advanced oxidation processes. Titanium dioxide has been intensively investigated since Fujishima and Honda discovered the photocatalytic splitting of water on titanium dioxide electrodes [3]. Titanium dioxide can be produced in various forms such as anatase, rutile, and brookite. The anatase phase of titanium dioxide shows better photoactivity than the rutile phase and is the most preferable material for the photocatalytic process due to its high photosensitivity, nontoxic nature, stability, and large band gap [4–6]. Titanium dioxide is an n-type semiconductor with a band gap of 3.2 eV. It is worth mentioning that anatase titanium dioxide absorbs only wavelengths in the near-UV region ($\lambda \leq 390$ nm), which constitutes about 3% of the solar spectrum. Therefore, solar energy cannot be utilized efficiently in real applications [7]. The coupling of titanium dioxide with another semiconductor oxide with a smaller band gap is a promising way to overcome this limitation. The photocatalytic efficiency and functionality can be improved by coupling a second semiconductor to titanium dioxide [8]. For instance, the photocatalytic properties of titanium dioxide were greatly enhanced by coupling with ZnO and CdS [9, 10]. The coupling of titanium dioxide with cadmium oxide (CdO) has not yet been reported in the literature for the degradation of dye stuffs. CdO is an n-type semiconductor with direct band gap of 2.5 eV, an indirect band gap of 1.98 eV and a melting point of 1,500 °C [11–16]. CdO nanostructures have low ohmic resistivity and high optical transmittance, with a moderate

refractive index (2.49) [17–19], which offers excellent properties for applications in optoelectric devices such as transparent electrodes [20], photovoltaic cells [21], photo-transistors [22], and photo-diodes [23].

Electrospinning offers a facile technique to create high surface-to-volume area fibers where the fibers have diameters an order of magnitude smaller than those produced by conventional spinning techniques. Electrospinning is a process by which fiber diameters ranging from tens nanometers to several micrometers can be formed [24–26]. Electrospun nanofibers can have approximately double the surface area of continuous thin films [27].

In this work, the photocatalytic properties were enhanced by a novel coupling of titanium dioxide with CdO by the electrospinning technique and a single calcination. The prepared nanostructures were utilized as a photocatalyst to degrade methyl orange dye.

Experimental section

Materials

Cadmium acetate, methyl orange, and poly(vinyl acetate) (PVAc, MW = 500,000 g/mol) were obtained from Aldrich USA. *N*,*N*-dimethylformamide (DMF, 99.5 assay) was obtained from Showa, Co. Japan. Titanium (1 V) isopropoxide (Ti(Iso), 98.0 assay) was purchased from Junsei Co. Ltd., Japan. These materials were used without any further purification.

Characterization

The surface morphology of the nanofibers was studied with a JEOL JSM-5900 scanning electron microscope, JEOL Ltd., Japan. The phase and crystallinity were characterized by using a Rigaku X-ray diffractometer (Rigaku Co, Japan) with Cu Kα ($\lambda = 1.54056$ Å) radiation over a 2θ range of angles from 10 to 90°. High-resolution images and selected area electron diffraction patterns were observed with a JEOL JEM 2010 transmission electron microscope (TEM) operating at 200 kV, JEOL Ltd., Japan. Thermal gravimetric analysis (TGA) was performed with a Pyris1 TGA analyzer, Perkin Elmer Inc, USA. The concentration of the dye during the photodegradation study was investigated by spectroscopic analysis using an HP 8453 UV–Visible spectroscopy system, Germany. The spectra obtained were analyzed by the HP ChemStation software 5890 series.

Electrospinning setup

A sol–gel composed of Ti(Iso) and PVAc was prepared as follows: 4 g of PVAc (14% wt, in DMF) solution and 6 g of Ti(Iso) were mixed, and a few drops of acetic acid were added until the solution became transparent. This sol–gel was electrospun without adding cadmium acetate reagent to obtain pure titanium dioxide nanofibers. To prepare the Ti(Iso)/PVAc/CdAc nanofibers, the aforementioned solution was prepared, and 0.1 g of cadmium acetate was added to it. Furthermore, this solution was homogeneously mixed under stirred conditions for 10 min. A high-voltage power supply (CPS-60 K02V1, Chungpa EMT Co., Republic of Korea) was used as a source of the electric field. The sol–gel was supplied through a plastic syringe attached to a capillary tip. A copper wire originating as the positive electrode (anode) was inserted into the sol–gel, and the negative electrode (cathode) was attached to a metallic collector covered with a polyethylene sheet. Both solutions (Ti(Iso)/PVAc with and without cadmium acetate) were briefly electrospun at 6 kV and a 15 cm working distance (the distance between the needle tip and the collector). The nanofiber mats formed were initially dried for 24 h at 80 °C under vacuum and then calcined in air at 500 °C for 1 h, with a heating rate of 5 °C/min.

The photocatalytic degradation of methyl orange dye in the presence of pure titanium dioxide and (TiO_2/CdO) nanofibers was carried out in a simple photo-reactor. The reactor was made of glass (1,000 mL capacity, 23 cm in height, and 15 cm in diameter), covered with aluminum foil and equipped with an ultra-violet lamp emitting source at a wavelength of 365 nm. The initial dye solution and the photocatalyst were placed in the reactor and continuously stirred for complete mixing during the photocatalytic reaction. Typically, 100 mL of dye solution (10 ppm concentration) and 50 mg catalyst were used. At specific time intervals, 2 mL samples were withdrawn from the reactor and centrifuged to separate the residual catalyst, and then the absorbance intensity was measured at the corresponding wavelength.

Results and discussions

Characterization of pristine titanium dioxide nanofibers

Figure 1a shows the SEM image of the dried Ti(Iso)/PVAc nanofibers [28]. It is clear from this figure that smooth and continuous nanofibers were produced by the electrospinning technique. Figure 1b shows the SEM image of the Ti(Iso)/PVAc nanofibers after calcination at 500 °C. These nanofibers have smaller diameters as compared to the dried nanofibers due to elimination of the polymer content at high temperature. These nanofibers still maintained their one-dimensional texture, indicating that the removal of PVAc and calcination at 500 °C did not damage the one-dimensional morphologies. Figure 1c shows the XRD

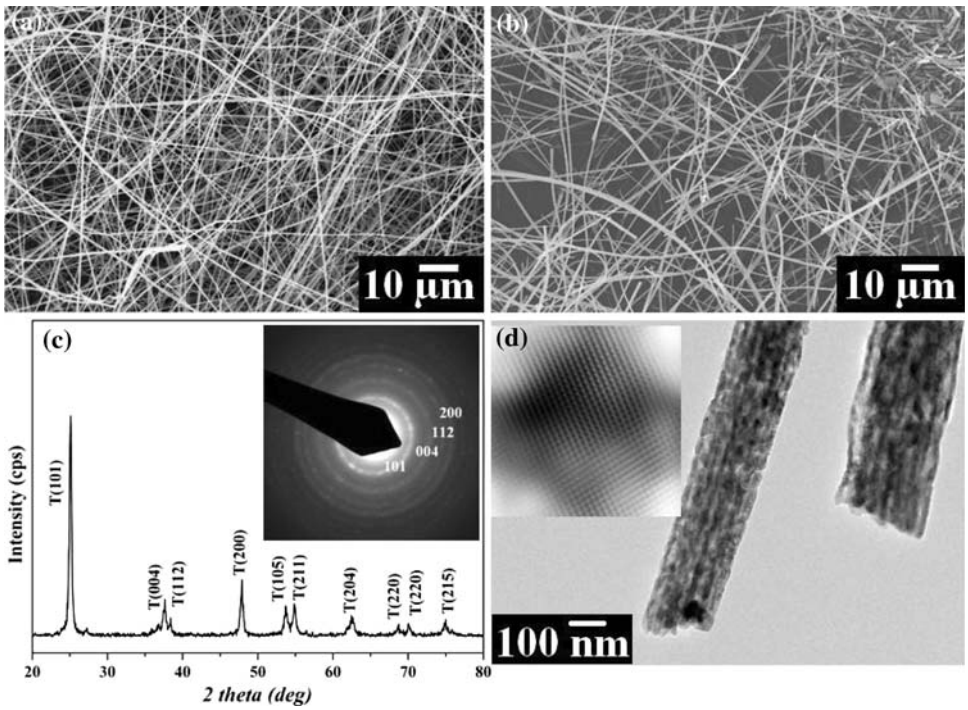

Fig. 1 SEM images before (**a**) and after (**b**) calcinations; XRD spectra and corresponding SAED inset (**c**). TEM image and FFT pattern (**d**) of Ti(Iso)/PVAc nanofibers after calcination at 500 °C for 1 h

pattern of Ti(Iso)/PVAc nanofibers after calcination at 500 °C. As shown in this spectra, the existence of strong diffraction peaks at 2θ values of 25.02, 37.68, 38.43, 47.90, 53.66, 54.82, 62.11, 68.78, 70.30, and 75.02 correspond to the crystal planes (101), (004), (112), (200), (105), (211), (204), (220), (220), and (215), respectively, indicating the formation of the anatase titanium dioxide [JCPDS card no 21-1272]. The inset in Fig. 1c shows the SAED pattern of the titanium dioxide nanofibers. There are no dislocations or stacking faults observed in the lattice planes, which confirms the good crystallinity of the synthesized nanofibers. The *d* spacing at 3.52, 2.37, 2.33, and 1.90 Å can be indexed to the (101), (004), (112), and (200) planes, which are close to the XRD results. Figure 1d shows the low-magnification TEM observation of titanium dioxide nanofibers after calcination at 500 °C and reveals an exact, fiber shaped, and smooth morphology. The inset in Fig. 1d shows the inverse fast Fourier transformation (FFT) image, which also confirms the good crystallinity in accordance with the SAED patterns.

Characterization of (TiO_2/CdO) nanofibers

Figure 2a and b shows SEM images of the dried Ti(Iso)/PVAc/CdAc nanofibers at low and high magnifications. As can be clearly seen, nanofibers with good morphologies are produced by the electrospinning of the prepared sol. It is clear from these figures that the addition of cadmium acetate did not affect the morphologies of the nanofibers; at regular shape and absence of beads was observed. Thus, these SEM images indicate that the electrospinning was performed properly.

In order to estimate the appropriate calcination temperature, the thermal behavior of Ti(Iso)/CdAc/PVAc composite fibers was investigated by TGA. Figure 2c shows the TGA results, and the first derivative curve was plotted to extract the useful information precisely, as shown in this figure. There are three exothermic peaks observed in the first derivative plot. The first peak at 60 °C might be explained as the evaporation of the moisture in the sample. According to thermal properties of CdAc and Ti(Iso) the peak at 278 °C can simultaneously be the decomposition of CdAc to CdO and Ti(Iso) to titanium dioxide, and the last peak at 490 °C corresponds to the elimination of PVAc polymer. Thus, the calcination temperature should be more than 490 °C, as there is no change in sample weight indicating the formation of pure inorganic oxide.

Figure 3 depicts the SEM images of Ti(Iso)/PVAc/CdAc after calcination at 500 °C for 1 h. Figure 3a and b shows the resultant SEM images at low and high magnification, respectively. As can be seen, the calcination of the nanofiber mats resulted in a decrease of the average diameter of the nanofibers as compared to the dried ones. Decreasing the nanofiber diameter can be explained by the removal of the polymer by calcination at high temperature. To practically investigate the effect of the addition of cadmium acetate, the surface area of both fibers (pristine titanium dioxide and TiO_2/CdO) was measured using the Brunauer–Emmett–Teller (BET) technique (ASAP 2010

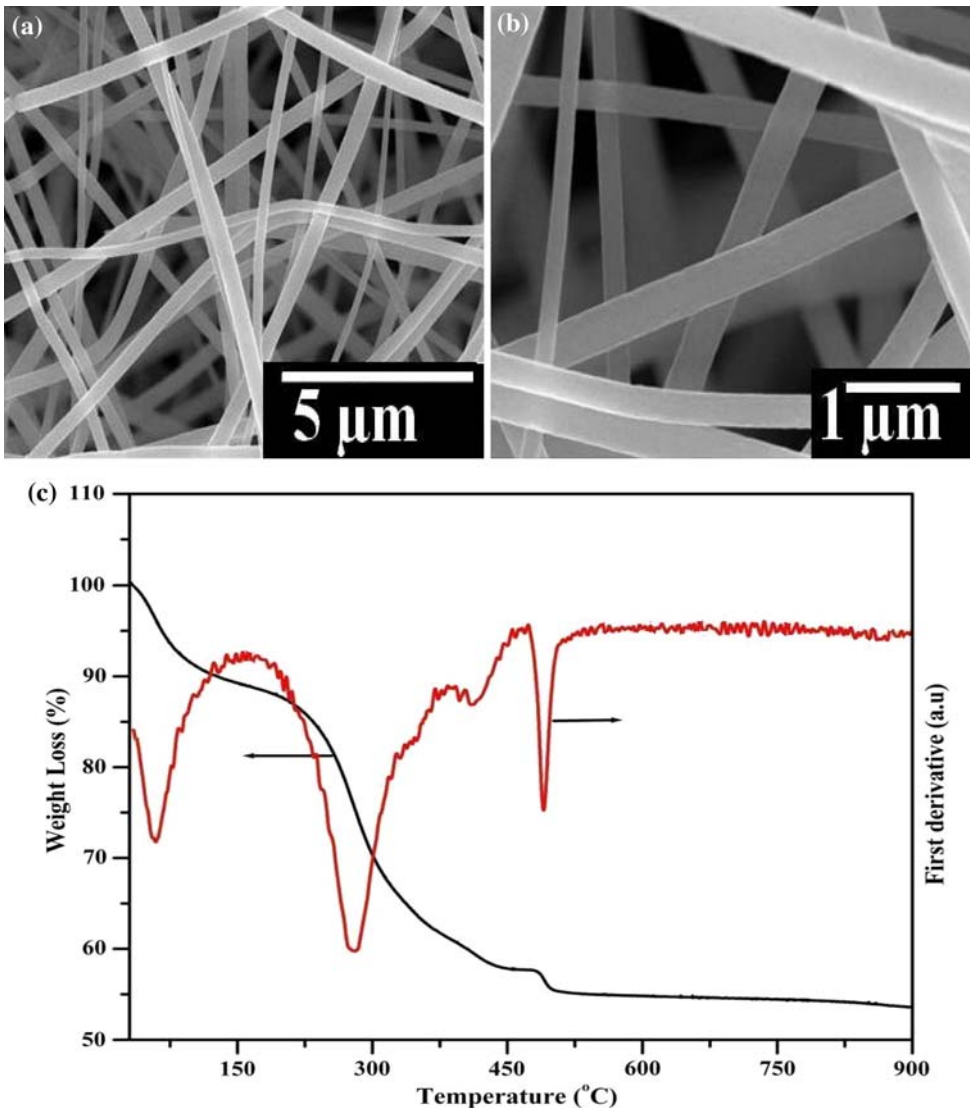

Fig. 2 SEM images of dried nanofibers at low and high magnifications (**a** and **b**); TGA results in oxygen atmosphere (**c**) of the Ti(Iso)/PVAc/CdAc after calcination at 500 °C for 1 h

micromeritics, USA). The results support the SEM images: the average surface area of the cadmium acetate-free nanofibers was about 21.3102 ± 0.1351 m^2/g, while it was 65.3067 ± 0.4677 m^2/g for the nanofibers obtained from the calcination of Ti(Iso)/PVAc/CdAc electrospun nanofiber mats. As can be concluded from these results, the surface area of the CdO containing nanofibers is more than three times that of the pure titanium dioxide nanofibers, which strongly enhance the photocatalytic activity.

XRD is a reliable technique for investigating the nature of any crystalline material. Figure 3c represents the XRD pattern of the nanofibers obtained after the calcination of Ti(Iso)/PVAc/CdAc mats. As shown in this spectrum, the results confirm formation of pure anatase titanium dioxide; the existence of strong diffraction peaks at 2θ values of 25.09, 47.10, 54.02, 62.73, 70.34, and 75.16 correspond to the crystal planes of (101), (200), (105), (204), (220), and (215), respectively, indicating the formation of anatase titanium dioxide [JCPDS card no. 21-1272]. However, in addition to these titanium dioxide peaks, the extra peaks at 2θ values of 37.99, 55.10, 68.803, and 82.793 correspond to the crystal planes (200), (220), (222), and (400), indicating the presence of the CdO [JCPDS card no. 05-0640]. To make it easy, in Fig. 3, we have marked the peaks corresponding to titanium dioxide and CdO as T and C, respectively. Overall, results confirm the formation of TiO_2/CdO nanofibers.

Figure 4 shows the X-ray photoelectron spectroscopy (XPS) results of the calcined nanofibers, and the binding energy was calibrated using the C 1s signal (284 eV) from the coating surface. The presence of a peak for the carbon 1s region is generally believed to be due to the presence of organic residue in the sample [29]. As shown in this figure, the Cd 3d region in CdO consists of the main $3d_{5/2}$ and $3d_{3/2}$ spin–orbit components at binding energies of 403 and 410 eV, respectively. In addition to 3d, we also observed

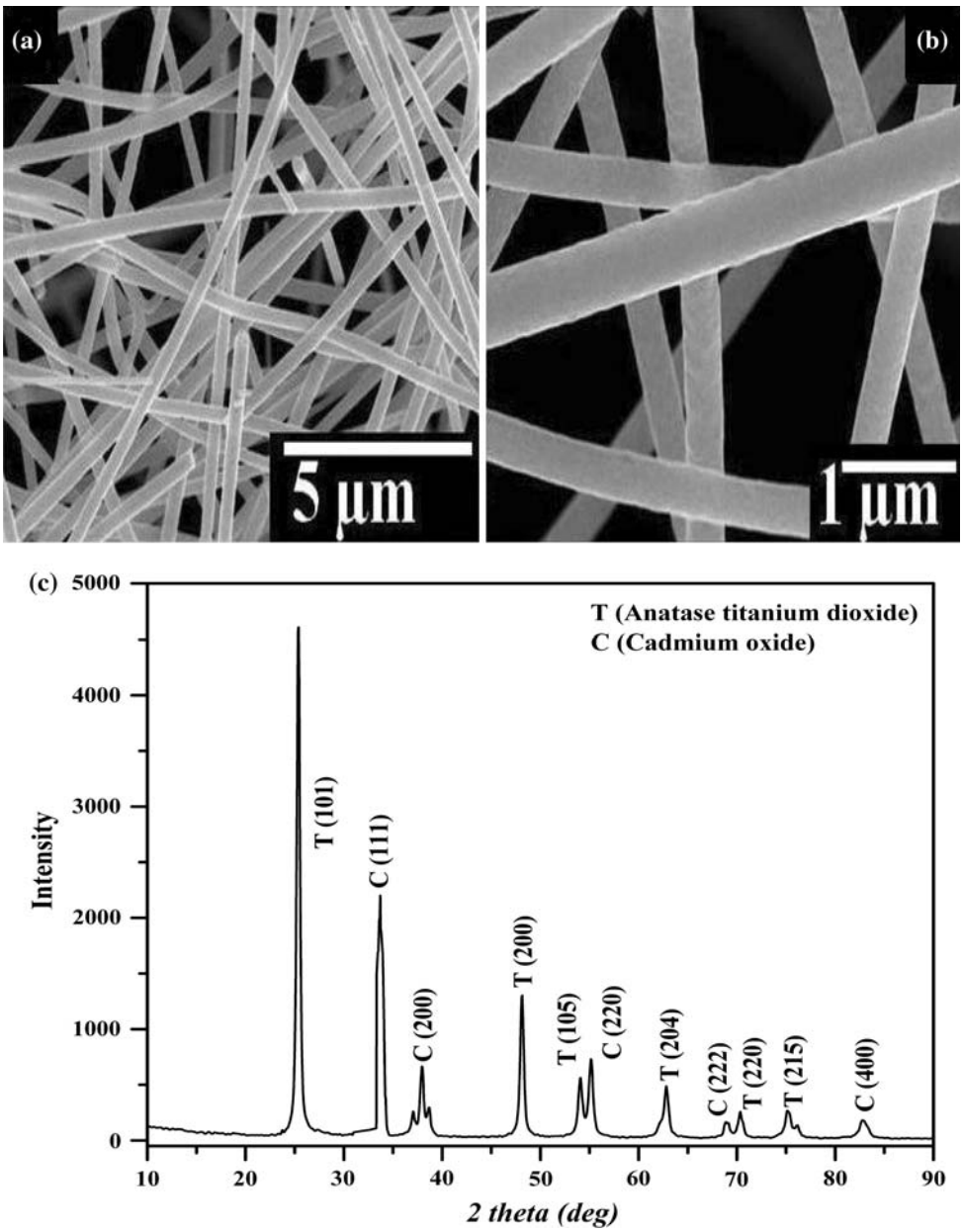

Fig. 3 SEM images at low and high magnifications (**a** and **b**); XRD spectra for the nanofibers obtained after calcination of Ti(Iso)/PVAc/CdAc nanofibers (**c**)

3p spin–orbit components for Cd at the binding energy of 617 eV. Similarly, the Ti 2p region in titanium dioxide consists of Ti $2p_{3/2}$ and Ti $2p_{1/2}$ spin–orbit components at binding energies of 457 and 465 eV, respectively. In addition to Ti 2p, we also observed 2s spin components for Ti at a binding energy of 565 eV. O 1s for oxygen is easily identified at a binding energy of 529 eV [29, 30].

Transmission electron microscopy (TEM) analysis can be used to differentiate between the crystalline and amorphous material structures. Structural characterization of the as-prepared (TiO_2/CdO) nanofibers is shown in Fig. 5. Figure 5a shows the low-magnification TEM observation of an exact fiber shape and smooth morphology, as proven by SEM analysis in density and dimensions. Figure 5b shows the high-resolution TEM image of the marked portion, which indicates that the distance between two consecutive planes is the same and that the atomic planes are uniformly arranged in parallel, which indicates good crystallinity. Moreover, different types of crystal planes with different distances between the successive planes can be observed in the figure, which might refer to the two oxides. It is noteworthy to mention that the inverse FFT image in the bottom inset of Fig. 5b also confirms good crystallinity, in accordance with HRTEM. The inset in Fig. 5b shows the SAED pattern of the same marked area. The *d* spacings of 3.52, 2.71, 2.35, and 1.90 Å can be indexed to the (101), (111), (200), and (200) planes, close to the XRD results. There are no dislocations or

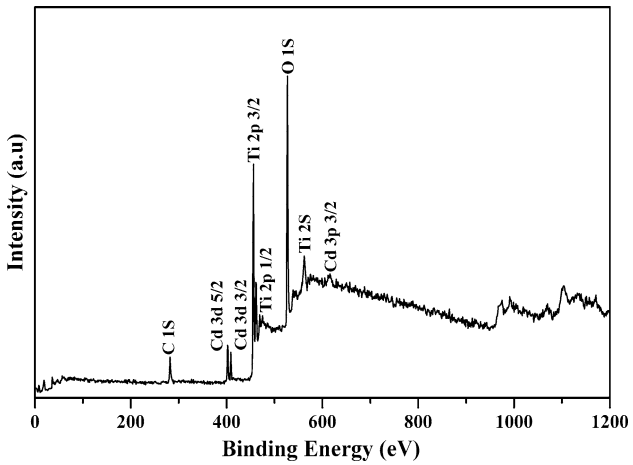

Fig. 4 The XPS spectrum confirming different cadmium and titanium states in addition to oxygen and carbon

imperfections observed in the lattice planes, which confirms the good crystallinity of the synthesized nanofibers.

Photocatalytic properties

Dye degradation is a well-known strategy to check the photocatalytic activity. In this study, we used methyl orange (MO), often used in titrations because of its clear color changes. The UV absorbance spectra for different concentrations of dye solutions (starting from 0.05 to 4 mg/L) were measured within the range of 325–575 nm. Figure 6a shows the results. Figure 6b represents the relationship between the dye concentration and the measured absorbance at 464 nm. The maximum measured intensities increase linearly with increasing dye concentration and for which the absorbance curves have a maximum value at 464 nm. Statistical analyses of this curve

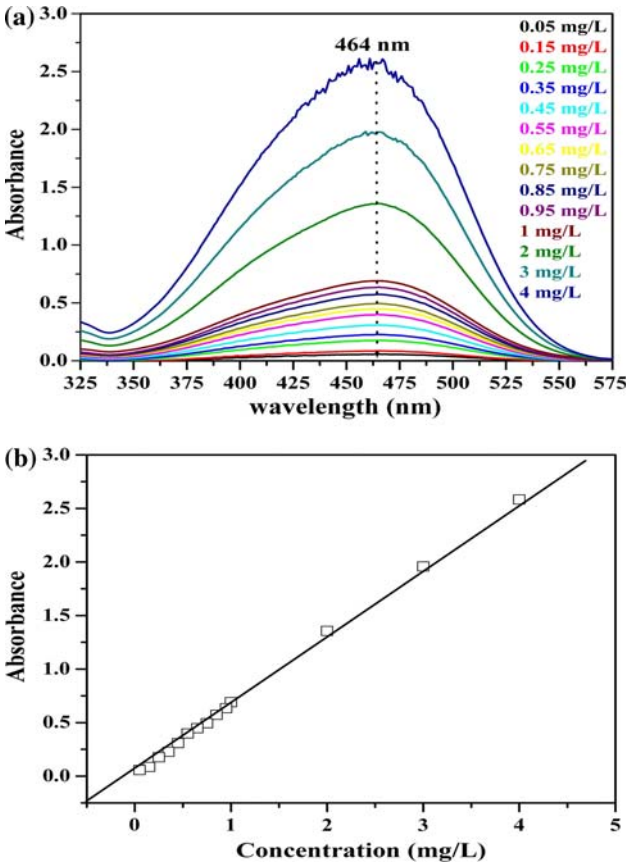

Fig. 6 Absorbance intensities for methyl orange dye solutions (**a**) and the relationship between the absorbance intensity and concentration of the dye at the optimum wavelength (**b**)

indicated the high accuracy of the linear model since the coefficient of determination R^2 of this model was 0.997, which reveals the good precision and reproducibility of this calibration curve. Consequently, during the photocatalytic activity investigation experiments, the concentration of the

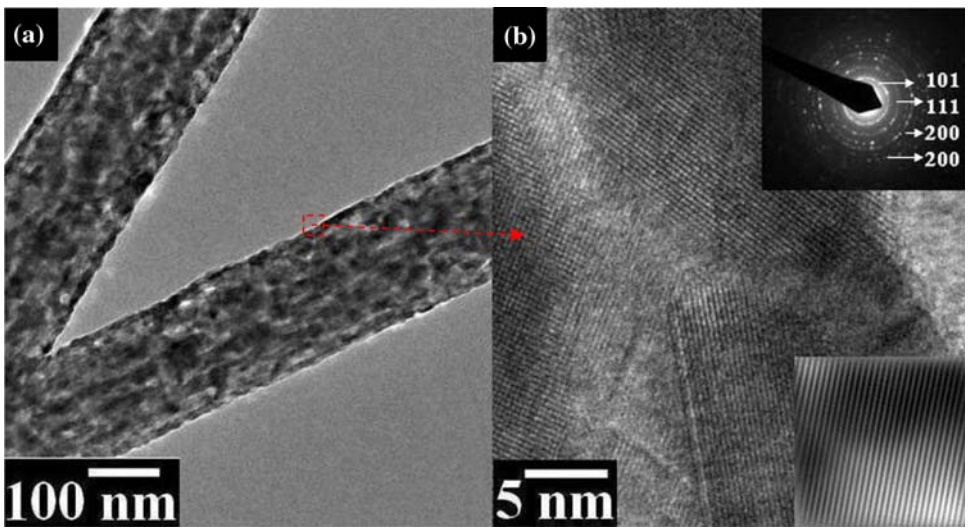

Fig. 5 TEM image (**a**) and high-resolution TEM (HRTEM) images (**b**) for the calcined nanofibers. The inset in (**b**) shows the SAED pattern of the marked areas in TiO_2–CdO main nanofibers

dye in any unknown sample was estimated by measuring the absorbance intensity at 464 nm and applying it to Fig. 6b.

To investigate the photocatalytic activity of the synthesized pure titanium dioxide and TiO_2/CdO nanostructures, these products were used individually as photocatalysts. The degradation of the utilized dye was carried out, and the results are presented in Fig. 7. It is clear from this figure that less than 50% of the MO dye was removed using pure titanium dioxide nanofibers, even after 180 min. However, in the case of TiO_2/CdO nanofibers, which show very good catalytic activity compared to pure titanium dioxide nanofibers, all the dye was oxidized within 75 min, as shown in Fig. 7.

The proposed mechanism for the enhanced photocatalytic activity of the TiO_2/CdO nanostructure photocatalyst is attributed mainly to the coupling effect of titanium dioxide and CdO. Figure 8 shows the mechanistic scheme for charge separation and the photocatalytic reaction of (TiO_2/CdO). The photo-generated electrons enter the conduction band of titanium dioxide from that of the excited conduction band of CdO. Similarly, the photo-generated holes are also transferred from the valence band of titanium dioxide to the valence band of CdO. This excellent charge separation enhances the lifetime of the charge carriers and enhances the efficiency of the interfacial charge transfer to the adsorbed substrates. Thus, the photocatalytic properties are enhanced because the possibilities of recombination between photo-generated electrons and holes are reduced by facilitating their separation [9].

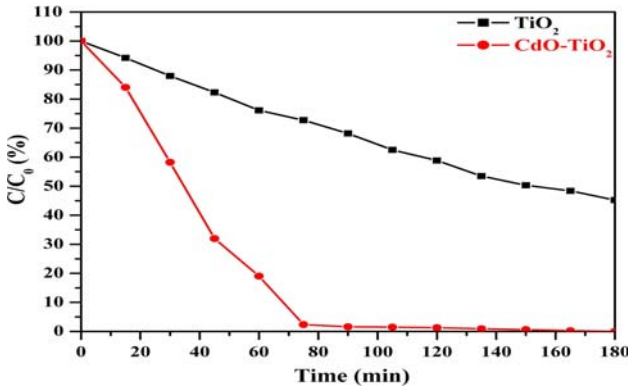

Fig. 7 Effect of pristine titanium dioxide nanofibers (TiO_2) and TiO_2–CdO nanofibers on the photocatalytic degradation of methyl orange dye

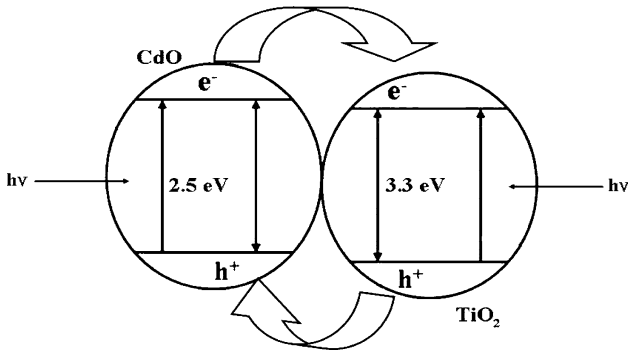

Fig. 8 A schematic diagram illustrating the principle of charge separation and photocatalytic activity for the TiO_2–CdO system

Conclusion

In this work, the preparation of titanium dioxide coupled to CdO by electrospinning was reported. TGA can be used to find the optimum temperature for the calcination process. The pristine nanofibers were sintered at 500 °C, resulting in complete elimination of the polymer and the production of (TiO_2/CdO) nanofibers with a specific surface area of 65.3067 m^2/g. The new nanostructure shows very good performance in the degradation of dye stuff compared to pure titanium dioxide nanofibers.

Acknowledgements This work was supported by a grant from the Korean Ministry of Education, Science and Technology (The Regional Core Research Program/Center for Healthcare Technology & Development, Chonbuk National University, Jeonju 561-756 Republic of Korea). We thank Mr. T.S. Bae and J.C. Lim, KBSI, Jeonju Branch, and Mr. Jong-Gyun Kang, Centre for University Research Facility, for taking the high-quality FE-SEM and TEM images, respectively.

References

1. Xia YN, Yang PD, Sun YG, Wu YY, Mayers B, Gates B, Yin YD, Kim F, Yan HQ (2003) Adv Mater 15:353
2. Lieber CM, Wang ZL (2007) Mater Res Bull 32:99
3. Honda K, Fujishima A (1972) Nature 238:37
4. Xu MW, Bao SJ, Zhang XG (2005) Mater Lett 59:2194
5. Mrowetz M, Selli E (2004) J Photochem Photobiol A 162:89
6. Beydoun D, Amal R (2002) Mater Sci Eng B 94:71
7. Ho W, Yu JC (2006) J Mol Catal A Chem 247:268
8. Bessekhouad Y, Chaoui N, Trzpit M, Ghazzal N, Robert D, Weber JV (2006) J Photochem Photobiol A 183:218
9. Kanjwal MA, Barakat NAM, Sheikh FA, Park SJ, Kim HY (2009) Macromol Res, in press
10. Bazargan AM, Fateminia SMA, Ganji ME, Bahrevar MA (2009) Chem Eng J 155:523
11. Ortega M, Santana G, Morales AA (2000) Solid State Electron 44:1765
12. Gurumurugan K, Mangalaraj D, Narayandass KS, Sekar K, Girija Vallabhan CP (1994) Semicond Sci Technol 9:1827
13. Dong W, Zhu C (2003) Opt Mater 22:227
14. Wu X, Wang R, Zou B, Wang L, Liu S, Xu J, Huang WJ (1998) Mater Res 13:604
15. Srivastava AK, Pandey S, Sood KN, Halder SK, Kishore R (2008) Mater Lett 62:727
16. Wang SH, Yang SH (2001) Mater Sci Eng C 16:37
17. NG V, Ahmed H, Shimada H (1998) Appl Phys Lett 73:972
18. Chernoutsan K, Dneprovskii V, Gavrilov S, Gusev V, Muljarov E, Romanov S, Syrnicov A, Shaligina O, Zhukov E (2002) Physica E 15:111

19. Benko FA, Koffyberg FP (1986) Solid State Commun 57:901
20. Champness CH, Ghoneim K, Chen (1985) Can J Phys 63:767
21. Su LM, Grote N, Schmitt F (1984) Electron Lett 20:716
22. Kondo R, Okimura H, Sakai Y (1971) Jpn J Appl Phys 10:1547
23. Drew C, Liu X, Ziegler D, Wang X, Bruno FF, Whitten J, Samuelson LA, Kumar J (2003) Nano Lett 3:143
24. Li D, Xia YN (2004) Adv Mater 16:1151
25. Li D, McCann JT, Xia YN (2006) J Am Ceram Soc 89:1861
26. Greiner A, Wendorff JH (2007) Angew Chem Int Ed 46:5670
27. Viswanathamurthi P, Bhattarai N, Kim CK, Kim HY, Lee DR (2004) Inorg Chem Commun 7:679
28. Kanjwal MA, Barakat NAM, Sheikh FA, Khil MS, Kim HY (2009) Int J Appl Ceram Technol 1:X
29. Chang J, Mane RS, Ham D, Lee W, Cho BW, Lee JK, Han SH (2007) Electrochim Acta 53:695
30. Guillot J, Fabreguette F, Imhoff L, Heintz O, Marco de Lucas MC, Sacilotti M, Domenichini B, Bourgeois S (2001) Appl Surf Sci 177:268